



HAL
open science

Sensitivity of Ocean-Atmosphere Coupled Models to the Coupling Method : Example of Tropical Cyclone Erica

Florian Lemarié, Patrick Marchesiello, Laurent Debreu, Eric Blayo

► To cite this version:

Florian Lemarié, Patrick Marchesiello, Laurent Debreu, Eric Blayo. Sensitivity of Ocean-Atmosphere Coupled Models to the Coupling Method : Example of Tropical Cyclone Erica. 2014. hal-00872496v5

HAL Id: hal-00872496

<https://inria.hal.science/hal-00872496v5>

Preprint submitted on 17 Nov 2014 (v5), last revised 10 Dec 2014 (v6)

HAL is a multi-disciplinary open access archive for the deposit and dissemination of scientific research documents, whether they are published or not. The documents may come from teaching and research institutions in France or abroad, or from public or private research centers.

L'archive ouverte pluridisciplinaire **HAL**, est destinée au dépôt et à la diffusion de documents scientifiques de niveau recherche, publiés ou non, émanant des établissements d'enseignement et de recherche français ou étrangers, des laboratoires publics ou privés.

Sensitivity of ocean-atmosphere coupled models to the coupling method : example of tropical cyclone Erica

By Florian LEMARIÉ^{1*}, Patrick MARCHESIELLO², Laurent DEBREU¹ and Eric Blayo³,

¹*Inria, Univ. Grenoble Alpes, LJK, F-38000 Grenoble, France CNRS, LJK, F-38000 Grenoble, France*

²*LEGOS, IRD, Toulouse, France*

³*Univ. Grenoble Alpes, LJK, F-38000 Grenoble, France CNRS, LJK, F-38000 Grenoble, France, Inria*

(Manuscript received xx xxxx xx; in final form xxxxxx xx)

ABSTRACT

In this paper, the sensitivity of Atmospheric and Oceanic Coupled Models (AOCMs) to the coupling method is investigated. We propose the adaptation of a Schwarz-like domain decomposition method to AOCMs. We show that the iterative process of the method ensures consistency of the coupled solution across the air-sea interface, contrarily to usual *ad-hoc* algorithmic approaches. The latter are equivalent to only one iteration of a Schwarz-like iterative method, which does not provide a converged state. It is generally assumed that this lack of consistency does not affect significantly the physical properties of the solution. The relevancy of this statement is first assessed in a simplified problem, then in the realistic application of a mesoscale atmospheric model (WRF) coupled with a regional oceanic model (ROMS) to simulate the genesis and propagation of tropical cyclone Erica. Sensitivity tests to the coupling method are carried out in an ensemble approach. We show that with a mathematically consistent coupling the spread of the ensemble is reduced, suggesting that there is room for further improvements in the formulation of AOCMs at a mathematical and numerical level.

Keywords: ocean-atmosphere coupling, domain decomposition methods, air-sea interface, Schwarz algorithms.

* Corresponding author.

e-mail: florian.lemarie@inria.fr

1. Introduction

1.1. Context

Many applications in global/regional oceanography and meteorology require Atmospheric and Oceanic Coupled Models (AOCMs) which account for important air-sea feedbacks. Separate integrations of the oceanic and atmospheric numerical models in forced mode (i.e. without feedback from one component to the other) may be satisfactory for numerous applications and process studies (e.g. Marchesiello et al., 2003; Colas et al., 2012; Lemarié et al., 2012). However, two-way coupling is essential for analyzing energetic and complex phenomena like tropical cyclones (e.g. Bao et al., 2000; Jullien et al., 2014), eastern boundary upwellings (e.g. Perlin et al., 2007; Capet et al., 2008), and more generally climate trends (e.g. Large and Danabasoglu, 2006; Terray et al., 2011). In that case, connecting the two model solutions at the air-sea interface is an arduous task which jointly raises mathematical, physical and computational issues.

Besides the oceanic and atmospheric models, the formulation of AOCMs is based on several components: a parameterization of the turbulent air-sea fluxes, a coupling infrastructure, and a coupling algorithm. Several parameterizations for surface atmospheric flow dynamics under oceanic influence have been designed. Those parameterizations are derived at a semi-empirical level and are based on field and laboratory experiments designed to carefully tune the parameter values (Fairall et al., 2003; Large, 2006). As for computational issues, numerous coupling softwares were developed in the last decade (Hill et al., 2004; Joppich and Kürschner, 2006; Redler et al., 2010). Those tools are needed to handle message passing, synchronization in time and regridding procedures (i.e., interpolation/extrapolation) between the computational grids. The last ingredient, of numerical nature, in the design of an AOCM is a *consistent* coupling algorithm; this is the main subject of this paper. The notion of *consistency* associated with the ocean atmosphere coupling problem will be clarified below in Sec. 1.1.2..

It is known that coupled model solutions exhibit a strong sensitivity to model parameters (Bengtsson, 1999; McWilliams, 2007). More specifically, sensitivity to perturbations in the initial conditions (Ploshay and Anderson, 2002), coupling frequency (Lebeaupin Brossier et al., 2009; Terray et al., 2011; Masson et al., 2012), and to air-sea flux formulation (Lebeaupin Brossier

et al., 2008) have been reported, in addition to the sensitivity that is inherent to each component of the coupled system (Tribbia and Baumhefner, 1988). This is arguably a source of concern when it comes to assess the AOCMs solution. Uncertainties in the specification of air-sea fluxes is strongly related to the empirical nature of atmospheric surface layer parameterizations resulting from the extreme complexity of the physical processes that we wish to represent. In general, a given parameterization is designed and tuned for a particular geographical region or a particular range of static stability. A lot of efforts are being directed toward improving physical parameterizations because these are usually considered as the major source of errors in AOCMs. However, it is arguably crucial to keep working on other model developments and identify other possible sources of error/deficiency. Preliminary studies of the fifth phase of the Coupled Model Comparison Project (CMIP5) do not report significant improvements in biases in present-day climate compared to CMIP3 (e.g. Roehrig et al., 2013; Sen Gupta et al., 2013). This suggests that finer horizontal resolution is not sufficient to cure the aforementioned problems. There is clearly a need for a more complete understanding of what goes on in numerical coupled models, notably through a finer consideration of numerical methods and modeling assumptions. To our knowledge, no systematic sensitivity study of the algorithmic aspects of air-sea coupling has been reported. We investigate this sensitivity in the present paper, starting with the definition of the coupling problem.

1.2. Coupling Problem

We symbolically describe the oceanic and atmospheric circulation models by partial differential operators \mathcal{L}_{oce} and \mathcal{L}_{atm} corresponding to the systems of equations solved by numerical models. Traditionally, we consider the primitive equations in the ocean and the fully-compressible Euler equations in the atmosphere. On the computational domain $\Omega = \Omega_{\text{atm}} \cup \Omega_{\text{oce}}$ (with external boundaries $\partial\Omega_{\text{atm}}^{\text{ext}}$ and $\partial\Omega_{\text{oce}}^{\text{ext}}$, see Fig. A1), the integration over a time period $[0, \mathcal{T}]$ corresponds to

$$\begin{cases} \mathcal{L}_{\text{atm}} \mathbf{U}^a = f_{\text{atm}}, & \text{in } \Omega_{\text{atm}} \times [0, \mathcal{T}], \\ \mathcal{B}_{\text{atm}} \mathbf{U}^a = g_{\text{atm}}, & \text{in } \partial\Omega_{\text{atm}}^{\text{ext}} \times [0, \mathcal{T}], \\ \mathcal{F}_{\text{atm}} \mathbf{U}^a = \mathbf{F}_{\text{oa}}(\mathbf{U}^o, \mathbf{U}^a, \mathcal{R}), & \text{on } \Gamma \times [0, \mathcal{T}], \end{cases} \quad (1)$$

$$\begin{cases} \mathcal{L}_{\text{oce}} \mathbf{U}^{\circ} = f_{\text{oce}}, & \text{in } \Omega_{\text{oce}} \times [0, \mathcal{T}], \\ \mathcal{B}_{\text{oce}} \mathbf{U}^{\circ} = g_{\text{oce}}, & \text{in } \partial\Omega_{\text{oce}}^{\text{ext}} \times [0, \mathcal{T}], \\ \mathcal{F}_{\text{oce}} \mathbf{U}^{\circ} = \mathbf{F}_{\text{oa}}(\mathbf{U}^{\circ}, \mathbf{U}^{\text{a}}, \mathcal{R}), & \text{on } \Gamma \times [0, \mathcal{T}], \end{cases} \quad (2)$$

with appropriate boundary conditions provided through the boundary operators \mathcal{B}_{oce} and \mathcal{B}_{atm} (the initialization of coupled models is an open problem that is beyond the scope here). In (1) and (2), $\mathbf{U}^{\text{a}} = (\mathbf{u}_h^{\text{a}}, T^{\text{a}})^t$ and $\mathbf{U}^{\circ} = (\mathbf{u}_h^{\circ}, T^{\circ})^t$ are the state variables with \mathbf{u}_h the horizontal velocity and T the (potential) temperature, f_{atm} and f_{oce} are forcing terms. For the sake of simplicity, we focus on temperature and momentum, we do not include salinity and humidity in the continuous formulation of the problem (it is however included in the practical application discussed in Sec. 5.). The oceanic domain Ω_{oce} and the atmospheric domain Ω_{atm} have a common interface Γ (Fig. A1). \mathbf{F}_{oa} is a function allowing the computation of air-sea fluxes. This function, generally based on the atmospheric surface layer similarity theory (e.g. Large, 2006), depends on \mathbf{U}^{a} and \mathbf{U}° in the vicinity of the air-sea interface (as shown in Fig. A1), and on a set of non-turbulent radiative fluxes \mathcal{R} .

In (1)-(2), the interface operators are defined as

$$\mathcal{F}_{\text{atm}\bullet} = \rho^{\text{a}} \mathbf{K}^{\text{a}} \partial_z \bullet, \quad \mathcal{F}_{\text{oce}\bullet} = \rho^{\circ} \mathbf{K}^{\circ} \partial_z \bullet,$$

where z is positive upward, ρ^{a} and ρ° are the densities of the fluids, and

$$\mathbf{K}^{\text{a}} = \begin{pmatrix} K_{\text{m}}^{\text{a}} \\ K_{\text{m}}^{\text{a}} \\ c_p^{\text{a}} K_{\text{t}}^{\text{a}} \end{pmatrix}, \quad \mathbf{K}^{\circ} = \begin{pmatrix} K_{\text{m}}^{\circ} \\ K_{\text{m}}^{\circ} \\ c_p^{\circ} K_{\text{t}}^{\circ} \end{pmatrix}.$$

We note K_{m}^{a} and K_{m}° the eddy viscosities, and K_{t}^{a} and K_{t}° the eddy diffusivities. The c_p terms correspond to the specific heat of the fluid.

In forced mode, \mathbf{U}° (resp. \mathbf{U}^{a} and \mathcal{R}) in (1) (resp. (2)) is provided offline by existing satellite-based or reanalysis products. In coupled mode, both models are run either simultaneously or successively on the same space-time interval. In this case, the consistency required

at the air-sea interface is the continuity of vertical fluxes¹

$$\begin{aligned} \rho^a K_m^a \partial_z \mathbf{u}_h^a &= \rho^o K_m^o \partial_z \mathbf{u}_h^o &= \boldsymbol{\tau} & \text{on } \Gamma \times [0, \mathcal{T}] \\ \rho^a c_p^a K_t^a \partial_z T^a &= \rho^o c_p^o K_t^o \partial_z T^o &= Q_{\text{net}} & \text{on } \Gamma \times [0, \mathcal{T}] \\ & & Q_{\text{net}} &= \mathcal{R} + Q_S \end{aligned}$$

where the surface wind stress $\boldsymbol{\tau}$ and the sensible heat flux Q_S (consequently the net heat flux Q_{net}) are computed using the function $\mathbf{F}_{\text{oa}} = (\boldsymbol{\tau}, Q_{\text{net}})^t$ previously introduced. The turbulent air-sea fluxes are given by a parameterization of the atmospheric surface layer. They usually take the form

$$\boldsymbol{\tau} = \rho^a C_D \|\Delta \mathbf{U}\| \Delta \mathbf{U}, \quad Q_S = \rho^a c_p^a C_H \|\Delta \mathbf{U}\| \Delta T, \quad (3)$$

where C_D and C_H are exchange coefficients that depend on surface roughness and local stability. $\Delta \mathbf{U}$ (resp. ΔT) correspond to the velocity (resp. temperature) jump across the air-sea interface which is defined, in a bulk way, as the region between the lowest vertical level in the atmospheric model and the shallowest vertical level in the oceanic model.

At this point we have defined all the necessary notations to formulate the coupled problem under study:

$$\begin{aligned} &\text{Find } \mathbf{U}^a \text{ and } \mathbf{U}^o \text{ that satisfy} \\ &\left\{ \begin{array}{ll} \mathcal{L}_{\text{atm}} \mathbf{U}^a &= f_{\text{atm}} & \text{in } \Omega_{\text{atm}} \times [0, \mathcal{T}] \\ \mathcal{B}_{\text{atm}} \mathbf{U}^a &= g_{\text{atm}} & \text{in } \partial \Omega_{\text{atm}}^{\text{ext}} \times [0, \mathcal{T}] \\ \mathcal{L}_{\text{oce}} \mathbf{U}^o &= f_{\text{oce}} & \text{in } \Omega_{\text{oce}} \times [0, \mathcal{T}] \\ \mathcal{B}_{\text{oce}} \mathbf{U}^o &= g_{\text{oce}} & \text{in } \partial \Omega_{\text{oce}}^{\text{ext}} \times [0, \mathcal{T}] \\ \mathcal{F}_{\text{atm}} \mathbf{U}^a &= \mathcal{F}_{\text{oce}} \mathbf{U}^o & \text{on } \Gamma \times [0, \mathcal{T}] \\ &= \mathbf{F}_{\text{oa}}(\mathbf{U}^o, \mathbf{U}^a, \mathcal{R}) \end{array} \right. \quad (4) \end{aligned}$$

for given initial and boundary conditions. It is worth mentioning that Lions et al. (1995) proved the existence of a global weak solution to problem (4) with interface conditions given by (3), considering that \mathcal{L}_{atm} and \mathcal{L}_{oce} are the primitive equations of the atmosphere and the ocean.

This paper is organized as follows. The existing coupling methods currently in use to solve (4) are presented in Sec. 2.. In Sec. 3., we provide critical comments about these methods

¹ Here, we assume wind-wave equilibrium, i.e., the atmospheric momentum flux to the wave field is immediately transferred to the ocean through wave breaking. The addition of a wave component to the coupling system would act as a low-pass filter to air-sea exchanges (see Sec.3.3.1. and Sec.6.)

and we introduce a new theoretical framework to solve the coupling problem. In Sec. 4. we present the formulation of our AOCM based on the Weather Research and Forecasting (WRF, Skamarock and Klemp, 2008) model and the Regional Oceanic Modeling System (ROMS, Shchepetkin and McWilliams, 2005). In Sec. 5. we assess the sensitivity of this model to the algorithmic approach for the simulation of a tropical cyclone. We show that a mathematically consistent algorithm leads to reduced stochasticity, i.e., less sensitivity of the coupled solution to perturbations in the initial condition and coupling frequency. We summarize and discuss our findings in Sec. 6..

2. A Classification of Existing Methods

Coupling methods can be categorized in two different groups : 1-way algorithms, when one model receive informations but does not send anything back to the other (e.g. Muller et al., 2007), and 2-way algorithms, when a feedback is introduced. We focus here on the latter. The usual coupling strategies can be found in Bryan et al. (1996) mostly for global configurations and in Bao et al. (2000) and Perlin et al. (2007) for regional high-resolution studies. A first algorithmic approach used for global problems is based on the exchange of averaged-in-time fluxes between the models (usually referred to as *asynchronous* coupling) whereas a second one deals with instantaneous fluxes (usually referred to as *synchronous* coupling). In this section, we expose the key differences between the two strategies.

2.1. Asynchronous Coupling by Time Windows (Based on Mean Fluxes)

Asynchronous coupling is the strategy used in most climate models of the IPCC². For this method, the total simulation time $[0, \mathcal{T}]$ is split into M smallest time windows $[t_i, t_{i+1}]$, i.e. $[0, \mathcal{T}] = \cup_{i=1}^M [t_i, t_{i+1}]$. The length of those time windows are typically between 1 hour and 1 day depending on target applications and the need to resolve or not the diurnal cycle. On a given time window, atmospheric and oceanic models only exchange time-averaged quantities. It has the advantage of requiring few communications between models. Noting $\langle \cdot \rangle_i$ a temporal

² Intergovernmental Panel on Climate Change

average on the time window $[t_i, t_{i+1}]$, the coupling algorithm is

$$\begin{cases} \mathcal{L}_{\text{atm}} \mathbf{U}^a = f_{\text{atm}} & \text{in } \Omega_{\text{atm}} \times [t_i, t_{i+1}] \\ \mathcal{F}_{\text{atm}} \mathbf{U}^a = \mathbf{F}_{\text{oa}}(\langle \mathbf{U}^o \rangle_{i-1}, \mathbf{U}^a, \mathcal{R}) & \text{on } \Gamma \times [t_i, t_{i+1}] \end{cases}$$

then

$$\begin{cases} \mathcal{L}_{\text{oce}} \mathbf{U}^o = f_{\text{oce}} & \text{in } \Omega_{\text{oce}} \times [t_i, t_{i+1}] \\ \mathcal{F}_{\text{oce}} \mathbf{U}^o = \langle \mathcal{F}_{\text{atm}} \mathbf{U}^a \rangle_i & \text{on } \Gamma \times [t_i, t_{i+1}] \end{cases} \quad (5)$$

This algorithm is schematically described in Fig. A2. First the atmospheric model is advanced from t_i to t_{i+1} using the averaged ocean state computed on the previous time window. Then, the fluxes used to force the atmospheric model are averaged and applied to the oceanic model on the same time interval (the fluxes are generally piecewise constant on each time window). This methodology ensures that over a time interval $[t_i, t_{i+1}]$ both models are forced by the exact same mean fluxes, implying a strict conservation of the quantities. Indeed, in both models the time integral of surface fluxes over the simulation equals $\langle \mathcal{F}_{\text{atm}} \mathbf{U}^a \rangle_{[0, \mathcal{T}]}$.

However, the solution of algorithm (5) is not rigorously solution of the original problem (4) because there is a synchronicity issue. The modification of the oceanic state \mathbf{U}^o on $[t_i, t_{i+1}]$ is not provided to the atmospheric component on the proper time interval $[t_i, t_{i+1}]$ but only on $[t_{i+1}, t_{i+2}]$. It is usually assumed that the loss of synchronization does not significantly impair the coupled solution, but we will show on the contrary that algorithm (5) leads to significant numerical errors (Sec. 3.3.2.).

2.2. Synchronous Coupling at the Time Step Level (Based on Instantaneous Fluxes)

In nature, the ocean and the atmosphere continuously exchange fluxes on scales ranging from global to micro scales. Therefore, proper coupling frequency between numerical models should be as small as possible, typically the largest time step between the oceanic and the atmospheric model. In this regard, a relevant algorithm would consist in exchanging instantaneous fluxes. Let us consider that the oceanic time step Δt_o is such that $\Delta t_o = N \Delta t_a$. The

corresponding algorithm reads

$$\left\{ \begin{array}{ll} \mathcal{L}_{\text{atm}} \mathbf{U}^a = f_{\text{atm}} & \text{in } \Omega_{\text{atm}} \times [t_i, t_i + N\Delta t_a] \\ \mathcal{F}_{\text{atm}} \mathbf{U}^a = \mathbf{F}_{\text{oa}}(\mathbf{U}^o(t_i), \mathbf{U}^a(t), \mathcal{R}(t)) & \text{on } \Gamma \times [t_i, t_i + N\Delta t_a] \end{array} \right. \quad (6)$$

$$\left\{ \begin{array}{ll} \mathcal{L}_{\text{oce}} \mathbf{U}^o = f_{\text{oce}} & \text{in } \Omega_{\text{oce}} \times [t_i, t_i + \Delta t_o] \\ \mathcal{F}_{\text{oce}} \mathbf{U}^o = \mathbf{F}_{\text{oa}}(\mathbf{U}^o(t_i), \mathbf{U}^a(t_i), \mathcal{R}(t_i)) & \text{on } \Gamma \times [t_i, t_i + \Delta t_o] \end{array} \right.$$

The oceanic and atmospheric components are integrated forward for a time period corresponding to Δt_o (or equivalently $N\Delta t_a$). Data exchange of instantaneous values is then performed and model integration continues for another Δt_o period of time. This process is repeated until the final forecast time (Fig. A3). In (6) the oceanic component receives instantaneous values from the atmosphere but integrated values can also be considered between t_i and $t_i + N\Delta t_a$ to avoid aliasing errors (Fig. A3,b). Both choices raise either conservation, aliasing or synchronization problems. In addition, algorithm (6) is difficult to implement efficiently from computational and numerical view points. Code communications are extremely frequent and time integration schemes must be carefully considered for consistent interfacial conditions.

At first glance, (6) may appear as a solution of the full problem (4). This is, however, formally true only in the limit $\Delta t_o, \Delta t_a \rightarrow 0$. Indeed, in most numerical models vertical diffusion is treated implicitly-in-time; air-sea fluxes are thus provided at time $t_i + \Delta t$ rather than t_i as in (6). As for algorithm (5), the loss of mathematical consistency due to numerical implementation may lead to significant errors (Sec. 3.3.2.).

3. Numerical and Physical Considerations

In the previous section, we showed that the numerical methods generally used to solve the coupled problem (4) are not fully satisfying from a mathematical point of view. In this section, we specify further the ocean-atmosphere coupling problem based on physical considerations, then we propose an alternative method to solve it.

3.1. Physical Constraints

Coupling methods used in the context of AOCMs differ from the methods usually used for multi-physics (fluid-fluid) coupling. However, the latter can not be easily applied to AOCMs

because they often assume a full representation of all the spatio-temporal scales involved in the problem. The oceanic and atmospheric variability is spectrally broad band across all scales from micro $\mathcal{O}(10^{-3} \text{ m}, 10^{-3} \text{ s})$ to global $\mathcal{O}(10^7 \text{ m}, 10^{10} \text{ s})$ scales. AOCMs contain essential parameterization to account for unresolved processes. The fluxes exchanged by the models are not the result of a discrete derivative in the vicinity of the air-sea interface but are given by atmospheric surface layer parameterizations based on the so-called bulk aerodynamic formulae. Bulk formulations are symbolically represented by the function F_{oa} in (4). They are defined and calibrated semi-empirically using measurements averaged in time over about an hour or more, and for a restricted range of stability values (Large, 2006). There is little knowledge and observations of air-sea fluxes at high temporal scales (see discussion in Danabasoglu et al. (2006), Sec. 2) and the sign of air-sea fluxes is uncertain on time scales less than 10 minutes. In addition, high frequency physical processes are associated with the wavy boundary layer that requires specific time-dependent equations to be solved (Bao et al., 2000). The wavy boundary layer tends to act as a low-pass filter on air-sea exchanges. Therefore and for all reasons mentioned above, we consider mean hourly fluxes preferable when using bulk formulations (see Large, 2006, for a discussion). A time-averaging procedure, acting as a smoother of smallest time scales, is thus adopted in algorithm (5). We consider that algorithm (6) is relevant only if additional physical processes predominant on short time-scales are explicitly addressed in the flux computation.

3.2. Numerical Considerations

We showed in Sec. 2. that usual coupling methods used in AOCMs are not entirely satisfactory with respect to consistency, conservation or synchronization. An illustration of numerical errors is given here based on a simplified one-dimensional coupling problem with an interface at $z = 0$:

$$\left\{ \begin{array}{ll} \partial_t q_2 - \partial_z(\nu_2 \partial_z q_2) = f_2, & \text{in }]0, L_2[\times]0, \mathcal{T}[, \\ q_2(L_2, t) = 0, & t \in [0, \mathcal{T}], \\ \nu_2 \partial_z q_2(0, t) = \nu_1 \partial_z q_1(0, t), & t \in [0, \mathcal{T}], \end{array} \right. \quad (7)$$

$$\left\{ \begin{array}{ll} \partial_t q_1 - \partial_z(\nu_1 \partial_z q_1) = f_1, & \text{in }]-L_1, 0[\times [0, \mathcal{T}], \\ q_1(-L_1, t) = 0, & t \in [0, \mathcal{T}], \\ q_1(0, t) = q_2(0, t), & t \in [0, \mathcal{T}]. \end{array} \right. \quad (8)$$

The complete setup for this simplified test-case is described in App. A, and a thorough mathematical and numerical study of this problem can be found in Lemarié et al. (2013a;b). We impose continuity of tracer q and its vertical flux at the interface. Fig. A4 (left panel) shows the ℓ_2 -norm of errors associated with synchronous and asynchronous methods. Note that we chose a testcase forced with right hand sides f_1 and f_2 which are identical whatever the coupling method. That is the reason why the coupling error does not grow significantly with time. It must be clear that setting $f_1 = f_2 = 0$ in (7-8) would lead to much larger errors constantly growing with time.

Based on purely numerical arguments, the synchronous method is preferable over the asynchronous one as it leads to much smaller error. However, because the synchronous method does not satisfy the aforementioned physical constraints (Sec. 3.3.1.) for coupling and also because of computational burden, we strive to propose an alternative approach which would theoretically prove more consistent.

3.3. Global in Time Schwarz Method

The Schwarz-like domain decomposition methods (see Gander, 2008, for a review) are widely used for coupling problems with different physics and/or different numerical treatment. Originally introduced for stationary problems, those methods have been recently extended to time-dependent problems to provide a global-in-time Schwarz method, a.k.a. Schwarz waveform relaxation (e.g. Gander and Halpern, 2007). The idea is to separate the original problem on $\Omega = \Omega_{\text{atm}} \cup \Omega_{\text{oce}}$ into subproblems on Ω_{atm} and Ω_{oce} , which can be solved separately. An iterative process is then applied to achieve convergence to the solution of the original problem. The main drawback of this approach is the iterative procedure which increases the computational cost of coupling, especially when convergence is slow (note that there is currently an active research aiming at optimizing the convergence speed of Schwarz-like methods; see discussion in Sec. 6.). These methods have already been applied to oceanic models for improving Poisson and Helmholtz solvers, open boundary specification and nesting techniques (Debreu and Blayo, 1998; Blayo and Debreu, 2006; Cailleau et al., 2008).

They also seem well suited to our ocean-atmosphere coupling problem (4). Using the notations introduced previously, the iterative algorithm on a time window $[t_i, t_{i+1}]$ can be written as follows (for a given initial condition at $t = t_i$):

$$\begin{aligned} & \text{Loop over } k \text{ until convergence} \\ & \left\{ \begin{array}{ll} \mathcal{L}_{\text{atm}} \mathbf{U}_k^{\text{a}} = f_{\text{atm}}, & \text{in } \Omega_{\text{atm}} \times [t_i, t_{i+1}] \\ \mathcal{F}_{\text{atm}} \mathbf{U}_k^{\text{a}} = \mathbf{F}_{\text{oa}}(\mathbf{U}_{k-1}^{\text{o}}, \mathbf{U}_k^{\text{a}}, \mathcal{R}_k), & \text{on } \Gamma \times [t_i, t_{i+1}] \\ \mathcal{L}_{\text{oce}} \mathbf{U}_k^{\text{o}} = f_{\text{oce}}, & \text{in } \Omega_{\text{oce}} \times [t_i, t_{i+1}] \\ \mathcal{F}_{\text{oce}} \mathbf{U}_k^{\text{o}} = \mathcal{F}_{\text{atm}} \mathbf{U}_k^{\text{a}}, & \text{on } \Gamma \times [t_i, t_{i+1}] \end{array} \right. \quad (9) \end{aligned}$$

where the subscripts k denotes the iteration number. The first guess $\mathbf{U}_{k=0}^{\text{o}}$ on $\Gamma \times [t_i, t_{i+1}]$ is generally taken from the converged solution on the previous time window $[t_{i-1}, t_i]$. The two models, at each iteration, are run successively: this is the so called *multiplicative* form of the algorithm. If the condition $\mathcal{F}_{\text{oce}} \mathbf{U}_k^{\text{o}} = \mathcal{F}_{\text{atm}} \mathbf{U}_k^{\text{a}}$ is replaced by $\mathcal{F}_{\text{oce}} \mathbf{U}_k^{\text{o}} = \mathcal{F}_{\text{atm}} \mathbf{U}_{k-1}^{\text{a}}$ both models can be run in parallel over the whole time window $[t_i, t_{i+1}]$: this is the *parallel* form of the algorithm. When convergence is reached, this algorithm gives the exact solution to (4). Note that with algorithm (9) the solution is independent of the size of time window $[t_i, t_{i+1}]$, as opposed to the asynchronous coupling method (akin to performing only one iteration of the Schwarz algorithm). However, for physical constraints on high-frequency treatment mentioned in Sec. 3.3.1., algorithm (9) should be modified to include time-averaging of the quantities near the air-sea interface as in (5):

$$\begin{aligned} & \text{Loop over } k \text{ until convergence} \\ & \left\{ \begin{array}{ll} \mathcal{L}_{\text{atm}} \mathbf{U}_k^{\text{a}} = f_{\text{atm}}, & \text{in } \Omega_{\text{atm}} \times [t_i, t_{i+1}] \\ \mathcal{F}_{\text{atm}} \mathbf{U}_k^{\text{a}} = \mathbf{F}_{\text{oa}}(\langle \mathbf{U}_{k-1}^{\text{o}} \rangle_i, \mathbf{U}_k^{\text{a}}, \mathcal{R}_k), & \text{on } \Gamma \times [t_i, t_{i+1}] \\ \mathcal{L}_{\text{oce}} \mathbf{U}_k^{\text{o}} = f_{\text{oce}}, & \text{in } \Omega_{\text{oce}} \times [t_i, t_{i+1}] \\ \mathcal{F}_{\text{oce}} \mathbf{U}_k^{\text{o}} = \langle \mathcal{F}_{\text{atm}} \mathbf{U}_k^{\text{a}} \rangle_i, & \text{on } \Gamma \times [t_i, t_{i+1}] \end{array} \right. \quad (10) \end{aligned}$$

Fig. A4 (right panel) shows that numerical errors using algorithm (10) are significantly reduced compared to the asynchronous method (5). Moreover, we numerically checked on a simple test case that algorithm (10) converges.

3.4. Partial Conclusion

We have so far discussed numerous subtleties of numerical and physical nature involved in the design of AOCMs. Before proceeding to a real-case study, we draw a few remarks

based on our survey of the algorithmic aspects of ocean-atmosphere coupling. Looking at (5) and (10), it appears that the asynchronous coupling method currently in use in global climate models corresponds to one iteration of the *multiplicative* form of a global-in-time Schwarz algorithm (Lemarié, 2008). In this respect, asynchronous coupling is mathematically inconsistent because it does not give the solution of the coupling problem (4) but an approximation. It can also easily be shown that the synchronous coupling (6) is equivalent to one iteration of a local-in-time Schwarz algorithm (Cai and Sarkis, 1998). As described above, it is possible to satisfy the required consistency at the expense of an iterative process.

To avoid the burden of the iteration process associated with Schwarz methods, a monolithic scheme (i.e. a single model including both the oceanic and atmospheric physics) may be used, but that would impose the ocean and atmosphere to be advanced on the same horizontal grid with the same time-step. This is unnatural in the case of space-time multi-physics problems. It must be clear that the Schwarz method does not interfere with the time-scale of physical processes. Convergence of the Schwarz method does not imply any instantaneous physical adjustment, e.g. of the oceanic boundary layer to the overlying atmospheric conditions. Its mode of action is on the mathematical consistency of the solution at the air-sea interface. It should not be confused with other iterative methods sometimes used in convective adjustment schemes or bulk formulations.

When using an iterative method, there are intertwined concerns : the computational cost and the convergence speed. The present paper is a preliminary study where attention is given to the relevancy of consistent methods, rather than their computational cost. However, one important question that first needs addressing is whether the Schwarz method actually converges in a practical application. We address this question in the next section by applying the *multiplicative Schwarz algorithm* to model the genesis and movement of tropical cyclone (TC) Erica in the southwest Pacific ocean during March 2003.

4. Model description and Experimental Setup

In this section we briefly present the numerical models composing our AOCM and our coupling strategy based on algorithm (10) and applied to tropical cyclone Erica.

4.1. Oceanic Model

The numerical oceanic model is ROMS (Shchepetkin and McWilliams, 2005) in its AGRIF-IRD³ version, see Shchepetkin and McWilliams (2009) for a description of the various ROMS kernels. ROMS is a split-explicit time stepping, hydrostatic, Boussinesq, free-surface primitive equation model specifically designed for regional applications. ROMS equations are formulated using a generalized terrain-following σ -coordinate, that can be configured to enhance resolution in the surface boundary layer at the air-sea interface. Our experiment is setup in a configuration with four open boundaries, 50 σ -coordinate levels (grid parameters are chosen to ensure that the surface grid-box depth is at most 1 m), a horizontal grid with $\Delta x = 1/3^\circ$, and $\Delta t = 1800\text{s}$. The domain roughly extends from 6°S to 25°S in latitude and from 142.5°E to 172.5°E in longitude (Fig. A5). Note that special care must be given to the numerical schemes for tracer transport to properly simulate this area of complex bathymetry (Marchesiello et al., 2009). Vertical mixing of tracers and momentum to predict $K_m^o(z)$ and $K_t^o(z)$ is done with the KPP parameterization (Large et al., 1994). The coupled simulations are conducted without any flux correction scheme nor sea-surface temperature or salinity restoring. Model initialization results from a ten-year spin-up simulation forced by climatological atmospheric fluxes provided by the Comprehensive Ocean-Atmosphere Dataset (COADS) fields and by the QuikSCAT Climatology of Ocean Winds (QuikCOW). The oceanic boundary conditions are interpolated from a climatology based on the SODA reanalysis (the forcing fields are constructed using the Romstools utilities, Penven et al. (2008)). Note that the spin-up simulation develops large intrinsic variability at the mesoscale that is uncorrelated at this scale with the actual motion (no data assimilation techniques were used). Our goal here is to document the solution sensitivity to the coupling methodology rather than provide the best possible hindcast.

4.2. Atmospheric Model

The atmospheric model used in our experiment is the WRF-ARW⁴ solver (Skamarock and Klemp, 2008). WRF integrates the fully compressible nonhydrostatic Euler equations formulated using a terrain-following mass vertical coordinate. The model grid has a horizontal

³ Adaptive Grid Refinement in Fortran-Institut de Recherche pour le Développement <http://www.romsagrif.org/>

⁴ Advanced Research WRF, <http://www.mmm.ucar.edu/wrf/users/>

resolution of $1/3^\circ$ with 31 vertical levels and the time step is 180s. The meteorological data used for model initialization and boundary conditions are the NCEP2 reanalysis⁵. Note that there was no need for bogus injection to initialize the generation of TC Erica, as is sometimes done for cyclone studies, because the initial perturbation was captured by the NCEP2 reanalysis. The physical options used for the present study are the WSM3 (WRF Single-Moment 3-class) scheme for microphysics, the Rapid Radiative Transfer Model for longwave radiation, the Dudhia shortwave radiation scheme, the 5-layer thermal-diffusion land-surface model, and the Betts-Miller-Janjic cumulus parameterization. The Planetary Boundary Layer scheme used to compute $K_m^a(z)$ and $K_t^a(z)$ is a non-local K-profile scheme (the Yonsei University (YSU) scheme, Hong et al. (2006)).

Similar WRF and ROMS configurations were used in an uncoupled mode in Jourdain et al. (2011) and Jullien et al. (2012) respectively to study the statistics of cyclonic activity over the South-Pacific, and the oceanic response to tropical cyclones. A following ROMS-WRF coupled study using our coupling method has recently been addressed (Jullien et al., 2014). The present study is focused on coupling rather than TC science.

4.3. Model Coupling Strategy

We implement a global-in-time Schwarz method to couple WRF and ROMS. In practice, the different steps corresponding to algorithm (10) on a given time window $[t_i, t_{i+1}]$ and for iteration k are :

- (i) Compute the atmospheric solution from t_i to t_{i+1} using \mathbf{U}_{k-1}^o (or $\mathbf{U}_{[t_{i-1}, t_i]}^o$ for $k = 1$)
- (ii) Send averaged air-sea fluxes $\langle \mathcal{F}_{\text{atm}} \mathbf{U}_k^a \rangle_i$ on $[t_i, t_{i+1}]$ to the oceanic model
- (iii) Integrate the oceanic model on the same time period (using $\mathcal{F}_{\text{atm}} \mathbf{U}_k^a(t_i)$ and $\langle \mathcal{F}_{\text{atm}} \mathbf{U}_k^a \rangle_i$, fluxes from t_i to t_{i+1} are linearly reconstructed; see Fig. A6)
- (iv) Send the newly computed \mathbf{U}_k^o to the atmospheric model.

Steps 1 to 4 are iteratively applied until convergence (or until a fixed number of iterations is attained). On each time-window $[t_i, t_{i+1}]$ the initial condition at $t = t_i$ corresponds to the converged solution from the previous time-window $[t_{i-1}, t_i]$. As mentioned earlier, one sequence of steps 1 to 4, without iterating, corresponds to (5).

⁵ National Center for Environmental Prediction, http://nomad3.ncep.noaa.gov/ncep_data/index.html

In our practical implementation, the turbulent components of air-sea fluxes are computed in the WRF surface layer scheme based on a classical similarity theory which uses stability functions from Paulson (1970), Dyer and Hicks (1970), and Webb (1970) to compute the surface transfer coefficients for heat, moisture, and momentum. For our experiments we consider the same horizontal grids in WRF and ROMS. This is not a limitation of our method but a choice to ensure that the focus is on coupling rather than interpolation/extrapolation errors.

4.4. Experimental Setup

Erica, a category 4 cyclone (on the Australia and Fiji scale), was generated in March 2003 off Australia and reached New Caledonia a few days later causing human and material damage on the island. This event was poorly forecast as various attempts gave a totally different track than observed. As a result the local alert system failed. Cyclone track prediction has improved in the last decade but large uncertainties remain, in part due to the neglect of ocean and atmosphere coupling (Bender et al., 1993). Latent heat release to the atmosphere is the source of cyclone intensity but TC-induced cooling of the surface ocean is a powerful negative feedback affecting both intensity and trajectory (Jullien et al., 2012; 2014). Representing the correct two-way interaction between sea surface temperature (SST) and tropical cyclones is thus of primary importance to cyclogenesis.

The present study is designed to check the viability of the Schwarz method in a strong coupling case and to address two important questions, namely the convergence properties of the method in a fully realistic framework and the impact of the coupling method on the coupled solution. Our analysis focuses on the inter-comparison between coupling strategies rather than the direct comparison with observations. The coupled model is not optimally tuned for that. The default bulk coefficients in WRF are not set for extreme events and wave age effects are neglected in the absence of a coupled wave model. In addition, TC intensity is underestimated here as horizontal grid spacing of more than 2-3 km cannot explicitly solve eyewall dynamics (including vortex Rossby waves and mesovortices) with consequences on the intensity of ascent surrounding the eye, warming of the core and associated cyclonic intensity (Gentry and Lackmann, 2009; Hill and Lackmann, 2009). Nevertheless, our simulations of Erica are realistic enough for the task at hand as it reproduces the observed intensity and track with some accuracy (see Fig. A10).

4.5. Ensemble Design and Simulation Strategy

Let us now describe the ensemble design. We restrict our model comparison to that between the asynchronous (5) and the Schwarz (10) methods. The synchronous coupling method (at the time-step level) is cumbersome and tedious to implement. In addition, as explained earlier, current parameterizations are inadequate for this type of coupling.

AOCMs tends to exhibit strong sensitivity to model parameters like the initial condition and/or the coupling frequency (Sec. 1.). To check whether part of this sensitivity is related to coupling consistency errors (rather than stochasticity), we design two ensembles of 18 members, one for each coupling method. The 18 members are generated through perturbations of initial conditions and coupling frequency. We consider time windows of 3 hours and 6 hours, and three different initial conditions are chosen for the atmospheric and the oceanic models. The atmospheric model is started either from Feb. 28, March 1 or March 2, corresponding to distinct synoptic setting (Fig. A7). As for the oceanic model, three initial conditions for the month of March are selected from the 10 year climatological spin-up. All coupled simulations cover the duration of cyclonic event, ending in March 16, 2003. For the ensemble integrated using the Schwarz method we systematically proceed to $M = 9$ iterations. This is done to avoid choosing an arbitrary stopping criterion, and to keep the computational cost at a reasonable level.

5. Numerical results

5.1. Convergence Properties

First, it is natural to check the behavior of the coupled solution with respect to the iterations when the Schwarz method is used. To do so, we introduce a convergence rate R_k using the sea surface temperature $\bar{T}^o(z = 0)$ averaged in time on a given time window. R_k is defined as the ratio between the ℓ_2 -norm of the error at two successive iterations, considering that the solution at iterate $k = M$ is the true solution of the problem :

$$R_k = \frac{\|e_k\|_2}{\|e_{k-1}\|_2} = \frac{\|\bar{T}_k^o(z = 0) - \bar{T}_M^o(z = 0)\|_2}{\|\bar{T}_{k-1}^o(z = 0) - \bar{T}_M^o(z = 0)\|_2},$$

$$\|e_k\|_2 = \sqrt{\sum_{i=1}^{n_x \times n_y} |(\bar{T}_k^o)_i(z = 0) - (\bar{T}_M^o)_i(z = 0)|^2}$$

with $\|\cdot\|_2$ the ℓ_2 -norm, and n_x (resp. n_y) the number of grid points in the zonal (resp. meridional) direction. For the algorithm to converge R_k must remain smaller than unity, and the smaller R_k the faster the convergence. In this study, it turned out that four iterations were usually sufficient for convergence (Fig. A8). However, the convergence speed of the method should depend on the model configuration and grid resolution. Finer resolution would lead to more energetic nonlinear effects which may impair the convergence speed of the method. These complications are left for a future study.

From a theoretical point of view, it is straightforward to show that Schwarz methods, and more generally iterative methods, are slower to converge in presence of low frequencies in the error as long as the problem under consideration is only weakly nonlinear. We can thus anticipate that the main differences in the coupled solutions integrated with Schwarz and asynchronous methods occur at low frequencies. Fig. A9 shows the temporal spectrum

$$\text{Sp}_\omega \{ \|\mathbf{u}_h^a(z = 10 \text{ m})_{k=M}\| - \|\mathbf{u}_h^a(z = 10 \text{ m})_{\text{asyn}}\| \}$$

of the difference between the coupling methods (\mathbf{u}_h^a being the solution obtained with the asynchronous method, i.e. one iteration only), with ω the frequency. As expected, the effect of iterations is primarily visible for low time-frequencies, which suggests that the Schwarz method would have a significant impact on large-scale and climate processes. Note that it is theoretically possible to design a Schwarz method which could converge equally fast at all frequencies (this is the so-called *Optimized Schwarz Method*). However, this method is tractable only for relatively simple academic problems and is not straightforward to generalize to the ocean-atmosphere coupling problem (see discussion in Sec. 6.).

5.2. Ensemble Spread

We checked that the Schwarz method converges at least in one realistic application of our coupled model system. Let us now illustrate the impact of the method on the robustness of the coupled solutions. Our analysis will focus on the cyclone track and intensity of each member of the two ensembles corresponding to the two coupling algorithms. We identify the cyclone track using minimum pressure at the first vertical level of the atmospheric model. The track envelop shown in Fig. A11 approximately follows the observed track with motion speed and underlying sea surface temperature in the same range (Fig. A10). It is striking that the dispersion of trajectories is significantly smaller for the ensemble based on the Schwarz method.

In this case, the maximum standard deviation is 164 km and the standard deviation is around 92 km compared to respectively 212 km and 125 km with the asynchronous method. Note that the track spread in both ensembles tend to reduce when approaching the south-east corner of the domain, presumably because all simulations share identical boundary conditions.

The same behavior as for cyclone track is manifest in time histories of the maximum surface wind speed (not shown), with a maximum deviation of 6.2 m s^{-1} for the asynchronous method compared to 3.7 m s^{-1} for the Schwarz method (3.7 m s^{-1} versus 2.2 m s^{-1} for the standard deviation). Therefore, two very important features of tropical cyclone events, namely their trajectory and intensity, are more robustly simulated when improving the consistency of coupling method.

6. Discussion and Conclusion

We have emphasized in this paper the key role of the coupling algorithm in the design of an atmospheric and oceanic coupled model. Very popular coupling methods used in regional and global climate models do not provide the exact solution to the ocean-atmosphere coupling problem (4), but an approximation. We introduced a natural and non-intrusive method to solve this problem and we showed its relevance. This method called Global-in-Time Schwarz Method is based on an iterative process. It can easily be shown that the usual synchronous (6) and asynchronous (5) methods prominent in climate models correspond to only one iteration of a Schwarz algorithm. However, the iterative procedure can substantially increase the computational cost of the AOCM (by a factor corresponding to the number of iterations to reach convergence).

A realistic application is produced by an ensemble of simulations through perturbations of the initial conditions and coupling frequency of a regional AOCM. The results suggest that part of the model sensitivity to perturbed parameters can be attributed to inaccuracies in the coupling method. Specifically, coupling inconsistencies can spuriously increase the physical stochasticity of atmospheric and oceanic events (materialized here by the ensemble spread). For our particular case, three iterations of the Schwarz method are sufficient to improve the coupled solutions with respect to the ensemble spread. We show that the iterative process should significantly modify the low-frequency component of the solution, whereas high-frequencies converge very rapidly. Therefore, we anticipate that the iterative procedure

would be particularly relevant to long-term climate studies. However, it remains to be seen how robust is the convergence regardless of the model formulation, particularly the boundary layer parameterizations at the air-sea interface. In this regard, the Schwarz algorithm can also be used as diagnostic tool to assess consistency between atmospheric and oceanic boundary layer parameterizations: two schemes could be recognized as *consistent* if they lead to a converging Schwarz algorithm.

For some applications, the computational cost of the Schwarz algorithm may be unaffordable and one would thus proceed to only one iteration of the method, thereby retrieving the asynchronous method. Based on our study and on our earlier theoretical work (Lemarié et al., 2013c;a;b), we can formulate some recommendations when the asynchronous coupling method is used :

- The coupling frequency (i.e. the size of time window between two exchanges) can be adequately set to minimize coupling errors and that of surface flux parameterizations. Because the Schwarz algorithm converges slowly at low-frequency, the shorter the time window the smaller the coupling error. However, because of large uncertainties in the specification of surface fluxes, the larger the time window the smaller the parameterization error. With those constraints and the requirement of a proper representation of the diurnal cycle, a coupling frequency between 1 and 3 hours would provide a good compromise. In addition, it is generally observed that the wave field acts as a low-pass filter on air-sea exchanges, with a cutoff around 2 hours, which suggests that a time window of 2 hours may be considered as a relevant choice.

- Lemarié et al. (2013a;b) show that the mathematical type of interface condition has great impact on the convergence speed of the Schwarz algorithm. In the case of a diffusion problem, replacing Dirichlet-Neumann⁶ conditions by a Robin (a.k.a. Fourier) interface condition (i.e., a linear combination of Dirichlet and a Neumann conditions) can dramatically improve the convergence speed if the weights in the linear combination are properly chosen. Even in the case of one single iteration of the method (i.e., the asynchronous method) coupling errors can be reduced by simply working on the type of interface condition. However, the theoretical

⁶ A Dirichlet condition amounts to specifying a value in the interface, whereas a Neumann condition amounts to specifying a flux.

problem is not straightforward for AOCMs because of bulk formulations. It is a work in progress.

APPENDIX A: One-Dimensional Diffusion Test Problem

In this section, we compare different coupling methods using a simple test case, which is assumed representative of an ocean-atmosphere type problem. To do so, we define two subdomains $\Omega_1 =]-L_1, 0[$ and $\Omega_2 =]0, L_2[$ with $L_1 = L_2 = 250$ m. In this example, we consider the one dimensional diffusion equation of a scalar quantity q

$$\partial_t q - \partial_z (\nu \partial_z q) = f, \quad (\text{A1})$$

with ν a diffusion coefficient such that $\nu = \nu_1$ in Ω_1 and $\nu = \nu_2$ in Ω_2 . We choose $\nu_1 \neq \nu_2$ to model the heterogeneous physical properties between the two subdomains. Uniqueness of solutions for the coupling problem is obtained with Dirichlet-Neumann conditions at $z = 0$ (i.e. we require the equality of the subproblems solutions and of their fluxes). The corresponding coupling problem reads

$$\left\{ \begin{array}{ll} \partial_t q_2 - \partial_z (\nu_2 \partial_z q_2) = f_2, & \text{in }]0, L_2[\times]0, \mathcal{T}[, \\ q_2(L_2, t) = \tilde{q}_2(t), & t \in [0, \mathcal{T}], \\ \nu_2 \partial_z q_2(0, t) = \nu_1 \partial_z q_1(0, t), & t \in [0, \mathcal{T}], \end{array} \right. \quad (\text{A2})$$

$$\left\{ \begin{array}{ll} \partial_t q_1 - \partial_z (\nu_1 \partial_z q_1) = f_1, & \text{in }]-L_1, 0[\times]0, \mathcal{T}[, \\ q_1(-L_1, t) = \tilde{q}_1(t), & t \in [0, \mathcal{T}], \\ q_1(0, t) = q_2(0, t), & t \in [0, \mathcal{T}], \end{array} \right. \quad (\text{A3})$$

for a given initial condition. We pose the problem to get analytical solutions of the form

$$q_2(z, t) = \frac{q_0}{8} \left[3 - \exp\left(-\frac{z}{\alpha_2}\right) \right] \left[1 + \cos^2\left(\frac{\pi t}{T}\right) \right]$$

$$q_1(z, t) = \frac{q_0}{8} \left[1 + \exp\left(\frac{z}{\alpha_1}\right) \right] \left[1 + \cos^2\left(\frac{\pi t}{T}\right) \right]$$

where the condition $\nu_2 \alpha_1 = \nu_1 \alpha_2$ is sufficient to ensure the proper regularity of the solution across the interface at $z = 0$. To obtain such analytical solutions, we set the right hand sides f_1 and f_2

$$f_1(z, t) = -\frac{q_0}{8} \left\{ \left(\frac{\pi}{T} \sin \frac{2\pi t}{T} \right) \left[1 + \exp\left(\frac{z}{\alpha_1}\right) \right] + \frac{\nu_1}{\alpha_1^2} \exp\left(\frac{z}{\alpha_1}\right) \left[1 + \cos^2\left(\frac{\pi t}{T}\right) \right] \right\},$$

$$f_2(z, t) = -\frac{q_0}{8} \left\{ \left(\frac{\pi}{T} \sin \frac{2\pi t}{T} \right) \left[3 - \exp\left(-\frac{z}{\alpha_2}\right) \right] - \frac{\nu_2}{\alpha_2^2} \exp\left(-\frac{z}{\alpha_2}\right) \left[1 + \cos^2\left(\frac{\pi t}{T}\right) \right] \right\}.$$

Equation (A1) is discretized using a backward Euler scheme in time and a second-order scheme on a staggered grid in space. The parameter values are $\alpha_1 = 50$, $\alpha_2 = 10$, $q_0 = 15$, $T_0 = 24 \times 3600$ s, $\nu_1 = 1$ m s⁻¹, $\nu_2 = 0.2$ m s⁻¹, $\Delta z = 1$ m, $\Delta t = 900$ s, and the total

simulation time is $\mathcal{T} = 2000$ days. To numerically solve the coupling problem (A2-A3), we use the six different methods described in the paper : the asynchronous method with instantaneous and averaged fluxes (the fluxes are reconstructed using a linear conservative scheme), the global-in-time Schwarz method with instantaneous and averaged fluxes, the synchronous method and the local-in-time Schwarz method. The global-in-time Schwarz method and the asynchronous method are integrated with time windows of 6 hours. As expected, the Schwarz methods (local or global in time) with instantaneous fluxes provide strictly the same solution $q^*(z, t)(z \in \Omega_1 \cup \Omega_2, t \in [0, \mathcal{T}])$ which is used as a reference to compute the ℓ_2 -norm of the error for other methods

$$\|\varepsilon(t_i)\|_2 = \sqrt{\sum_{k=1}^{k=N} |q(z_k, t_i) - q^*(z_k, t_i)|^2},$$

with N the number of grid points between $-L_1$ and L_2 . The time evolution of $\|\varepsilon\|_2$ is represented in Figure A4, and discussed in Sec. 33.2. and 33.3..

Acknowledgment

F. Lemarié and E. Blayo acknowledge the support of the French LEFE-MANU (Les Enveloppes Fluides et l'Environnement, méthodes MATHématiques et NUMériques) program through project COCOA (COUplage Côtes, Océan, Atmosphère). L. Debreu and P. Marchesiello were funded by the ANR through contract ANR-11-MONU-005 (COMODO). Authors are grateful to Gurvan Madec for helpful discussions and suggestions.

References

- J.-W. Bao, J.-M. Wilczak, J.K. Choi, and L.H. Kantha. Numerical simulations of air-sea interaction under high wind conditions using a coupled model : A study of hurricane development. *Mon. Weather Rev.*, 128(7):2190–2210, 2000.
- M. A. Bender, I. Ginis, and Y. Kurihara. Numerical simulations of tropical cyclone-ocean interaction with a high-resolution coupled model. *Journal of Geophysical Research-Atmospheres*, 98(D12):23245–23263, 1993.
- L. Bengtsson. From short-range barotropic modelling to extended-range global weather prediction: a 40-year perspective. *Tellus B*, 51(1): 13–32, 1999. ISSN 1600-0889.
- E. Blayo and L. Debreu. Nesting ocean models. In E. Chassignet and J. Verron, editors, *An Integrated View of Oceanography: Ocean Weather Forecasting in the 21st Century*. Kluwer, 2006.
- F.O. Bryan, B.G. Kauffman, W. G. Large, and P. R. Gent. The ncar csm flux coupler. Technical Report NCAR/TN-424+STR, NCAR, 1996.
- X.-C. Cai and M. Sarkis. Local multiplicative schwarz algorithms for steady and unsteady convection-diffusion equations. *East-West J. Numer. Math.*, 6:27–41, 1998.
- S. Cailleau, V. Fedorenko, B. Barnier, E. Blayo, and L. Debreu. Comparison of different numerical methods used to handle the open boundary of a regional ocean circulation model of the bay of biscay. *Ocean Modell.*, 25(1-2):1–16, 2008.
- X. Capet, F. Colas, J. C. McWilliams, P. Penven, and P. Marchesiello. Eddies in eastern-boundary subtropical upwelling systems. In M. Hecht and H. Hasumi, editors, *Ocean Modeling in an Eddying Regime*, volume 177 of *Geophysical Monograph Series*, page 350. American Geophysical Union, USA, 2008.
- F. Colas, J. C. McWilliams, X. Capet, and J. Kurian. Heat balance and eddies in the Peru-Chile Current System. *Clim. Dynam.*, 39(1-2): 509–529, 2012.
- G. Danabasoglu, W. G. Large, J. J. Tribbia, P. R. Gent, B.P. Briegleb, and J.C. McWilliams. Diurnal coupling in the tropical oceans of ccs3. *J. Climate*, 19(11):2347–2365, 2006.
- L. Debreu and E. Blayo. On the schwarz alternating method for oceanic models on parallel computers. *J. Comp. Phys.*, 141(2):93 – 111, 1998. ISSN 0021-9991.
- A. J. Dyer and B. B. Hicks. Flux-gradient relationships in the constant flux layer. *Quart. J. Roy. Meteorol. Soc.*, 96(410):715–721, 1970.
- C. W. Fairall, E. F. Bradley, J. E. Hare, A. A. Grachev, and J. B. Edson. Bulk parameterization of air-sea fluxes: updates and verification for the COARE algorithm. *J. Climate*, 16:571–591, 2003.
- M. J. Gander and L. Halpern. Optimized Schwarz waveform relaxation methods for advection reaction diffusion problems. *SIAM J. Numer. Anal.*, 45(2):666–697 (electronic), 2007. ISSN 0036-1429.
- M.J. Gander. Schwarz methods over the course of time. *Electron. Trans. Numer. Anal.*, 31:228–255, 2008.

- M.S. Gentry and G. M. Lackmann. Sensitivity of simulated tropical cyclone structure and intensity to horizontal resolution. *Monthly Weather Review*, 138(3):688–704, 2013/09/11 2009.
- C. Hill, C. DeLuca, V. Balaji, M. Suarez, and A. Silva. The Architecture of the Earth System Modeling Framework. *Computing in Science and Engg.*, 6:18–28, January 2004. ISSN 1521-9615.
- K. A. Hill and G. M. Lackmann. Analysis of idealized tropical cyclone simulations using the weather research and forecasting model: Sensitivity to turbulence parameterization and grid spacing. *Mon. Weather Rev.*, 137(2):745–765, 2009.
- S.-Y. Hong, Y. Noh, and J. Dudhia. A new vertical diffusion package with an explicit treatment of entrainment processes. *Mon. Weather Rev.*, 134:2318–2341, 2006.
- W. Joppich and M. Kürschner. MpCCI - a tool for the simulation of coupled applications. *Concurr. Comput. : Pract. Exper.*, 18:183–192, February 2006. ISSN 1532-0626. 10.1002/cpe.v18:2.
- N.C. Jourdain, P. Marchesiello, C.E. Lefèvre, E. Vincent, M. Lengaigne, and F. Chauvin. Mesoscale simulation of tropical cyclones in the south pacific : climatology and interannual variability. *J. Climate*, 24:3–25, 2011.
- S. Jullien, C. Menkès, P. Marchesiello, N. C. Jourdain, M. Lengaigne, A. Koch Larrouy, J. Lefevre, E. M. Vincent, and V. Faure. Impact of tropical cyclones on the heat budget of the South Pacific Ocean. *J. Phys. Oceanogr.*, 42:1882–1906, 2012.
- S. Jullien, P. Marchesiello, C. Menkès, J. Lefevre, N. C. Jourdain, G. Samson, and M. Lengaigne. Ocean feedback to tropical cyclones: climatology and processes. *Clim. Dynam.*, pages 1–24, 2014. 10.1007/s00382-014-2096-6.
- W. G. Large. Surface fluxes for practitioners of global ocean data assimilation. In E. Chassignet and J. Verron, editors, *An Integrated View of Oceanography: Ocean Weather Forecasting in the 21st Century*. Kluwer, 2006.
- W. G. Large and G. Danabasoglu. Attribution and impacts of upper-ocean biases in CCSM3. *J. Climate*, 19(11):2325–2346, 2006.
- W. G. Large, J. C. McWilliams, and S. C. Doney. Oceanic vertical mixing: A review and a model with a nonlocal boundary layer parameterization. *Rev. Geophys.*, 32(4):363–403, 1994.
- C. Lebeaupin Brossier, V. Ducrocq, and H. Giordani. Sensitivity of three mediterranean heavy rain events to two different sea surface fluxes parameterizations in high-resolution numerical modeling. *J. Geophys. Res.*, 113, 2008.
- C. Lebeaupin Brossier, V. Ducrocq, and H. Giordani. Effects of the air-sea coupling time frequency on the ocean response during mediterranean intense events. *Ocean Dyn.*, 59:539–549, 2009.
- F. Lemarié. *Algorithmes de Schwarz et couplage océan-atmosphère*. 2008. URL <http://tel.archives-ouvertes.fr/tel-00343501/en/>. Thesis (Ph.D.)–Grenoble University (France).
- F. Lemarié, J. Kurian, A. F. Shchepetkin, M. J. Molemaker, F. Colas, and J. C. McWilliams. Are There Inescapable Issues Prohibiting the use of Terrain-Following Coordinates in Climate Models ? *Ocean Modell.*, 42:57–79, 2012.
- F. Lemarié, L. Debreu, and E. Blayo. Toward an optimized global-in-time schwarz algorithm for diffusion equations with discontinuous and spatially variable coefficients, part 1 : the constant coefficients case. *Electron. Trans. Numer. Anal.*, 40:148–169, 2013a.
- F. Lemarié, L. Debreu, and E. Blayo. Toward an optimized global-in-time schwarz algorithm for diffusion equations with discontinuous and spatially variable coefficients, part 2 : the variable coefficients case. *Electron. Trans. Numer. Anal.*, 40:170–186, 2013b.
- F. Lemarié, L. Debreu, and E. Blayo. Optimal control of the convergence rate of schwarz waveform relaxation algorithms. *Lecture Notes in Computational Science and Engineering*, 91:599–606, 2013c.
- J.-L. Lions, R. Temam, and S. Wang. Mathematical theory for the coupled atmosphere-ocean models. *J. Math. Pures Appl.*, 74:105–163, 1995.
- P. Marchesiello, J. C. McWilliams, and A.F. Shchepetkin. Equilibrium structure and dynamics of the California Current System. *J. Phys. Oceanogr.*, 33(4):753–783, 2003.

- P. Marchesiello, L. Debreu, and X. Couvelard. Spurious diapycnal mixing in terrain-following coordinate models: The problem and a solution. *Ocean Modell.*, 26(3-4):159–169, 2009. 10.1016/j.ocemod.2008.09.004.
- S. Masson, P. Terray, G. Madec, J.-J. Luo, T. Yamagata, and K. Takahashi. Impact of intra-daily SST variability on ENSO characteristics in a coupled model. *Clim. Dynam.*, 39(3-4):681–707, 2012.
- J. C. McWilliams. Irreducible imprecision in atmospheric and oceanic simulations. *Proc. Natl. Acad. Sci.*, 104(21):8709–8713, 2007.
- H. Muller, F. Dumas, B. Blanke, and V. Mariette. High-resolution atmospheric forcing for regional oceanic model: the ivoire sea. *Ocean Dyn.*, 57:375–400, 2007.
- C A Paulson. The mathematical representation of wind speed and temperature profiles in the unstable atmospheric surface layer. *J. Appl. Meteorol.*, 9(6):857–861, 1970.
- P. Penven, P. Marchesiello, L. Debreu, and J. Lefèvre. Software tools for pre- and post-processing of oceanic regional simulations. *Environ. Mod. Software*, 23(5):660–662, 2008.
- N. Perlin, E. D. Skillingstad, R. M. Samelson, and P. L. Barbour. Numerical simulation of air-sea coupling during coastal upwelling. *J. Phys. Oceanogr.*, 37(8):2081–2093, 2007.
- J.J. Ploshay and J.L. Anderson. Large sensitivity to initial conditions in seasonal predictions with a coupled ocean-atmosphere general circulation model. *J. Geophys. Res.*, 29, 2002.
- R. Redler, S. Valcke, and H. Ritzdorf. OASIS4 - a coupling software for next generation earth system modelling. *Geoscientific Model Development*, 3(1):87–104, 2010.
- R. Roehrig, D. Bouniol, F. Guichard, F. Hourdin, and J.-L. Redelsperger. The present and future of the west african monsoon: a process-oriented assessment of cmip5 simulations along the amma transect. *J. Climate*, 2013. doi: <http://dx.doi.org/10.1175/JCLI-D-12-00505.1>.
- A. Sen Gupta, N.C. Jourdain, J.N. Brown, and Monselesan D. Climate drifts in the cmip5 models. *J. Climate*, 26:8597–8615, 2013.
- A. F. Shchepetkin and J. C. McWilliams. The Regional Oceanic Modeling System (ROMS): A split-explicit, free-surface, topography-following-coordinate ocean model. *Ocean Modell.*, 9(4):347–404, 2005.
- A. F. Shchepetkin and J. C. McWilliams. Correction and commentary for “Ocean forecasting in terrain-following coordinates: Formulation and skill assessment of the Regional Ocean Modelling System” by Haidvogel et al., *J. Comp. Phys.* 227, pp. 3595–3624. *J. Comp. Phys.*, 228(24):8985–9000, 2009.
- W. C. Skamarock and J. B. Klemp. A time-split nonhydrostatic atmospheric model for weather research and forecasting applications. *J. Comp. Phys.*, 227:3465–3485, 2008.
- P. Terray, Sebastien Masson, K. Kakitha, A. K. Sahai, and J.-J. Luo. The role of the frequency of SST coupling in the Indian Monsoon variability and monsoon-ENSO-IOD relationships in a global coupled model. *Clim. Dynam.*, 39(3-4):729–754, 2011.
- J. J. Tribbia and D. P. Baumhefner. The reliability of improvements in deterministic short-range forecasts in the presence of initial state and modeling deficiencies. *Mon. Weather Rev.*, 116:2276–2288, 1988.
- E. K. Webb. Profile relationships: The log-linear range, and extension to strong stability. *Quart. J. Roy. Meteorol. Soc.*, 96(407):67–90, 1970.

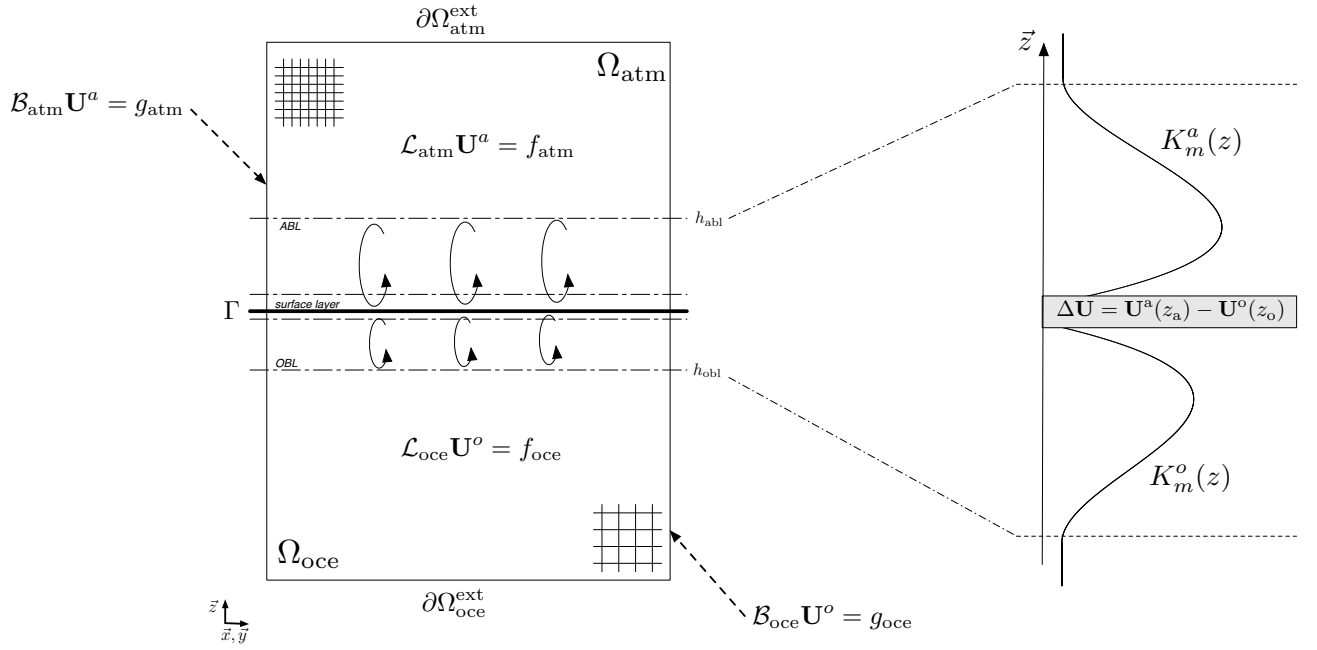


Fig. A1. Schematic view of the two non-overlapping subdomains Ω_{atm} and Ω_{oce} . The mathematical notations correspond to those introduced in Sec. 1.1.2.. The boundary layers encompassing the air-sea interface Γ and the atmospheric surface layer (gray shaded) are of particular importance for the coupling problem. The quantity $\Delta \mathbf{U} = \mathbf{U}^a(z_a) - \mathbf{U}^o(z_o)$ is directly involved in the computation of air-sea fluxes, with z_a (resp. z_o) the location of the lowest (resp. shallowest) vertical level in the atmospheric (resp. oceanic) model.

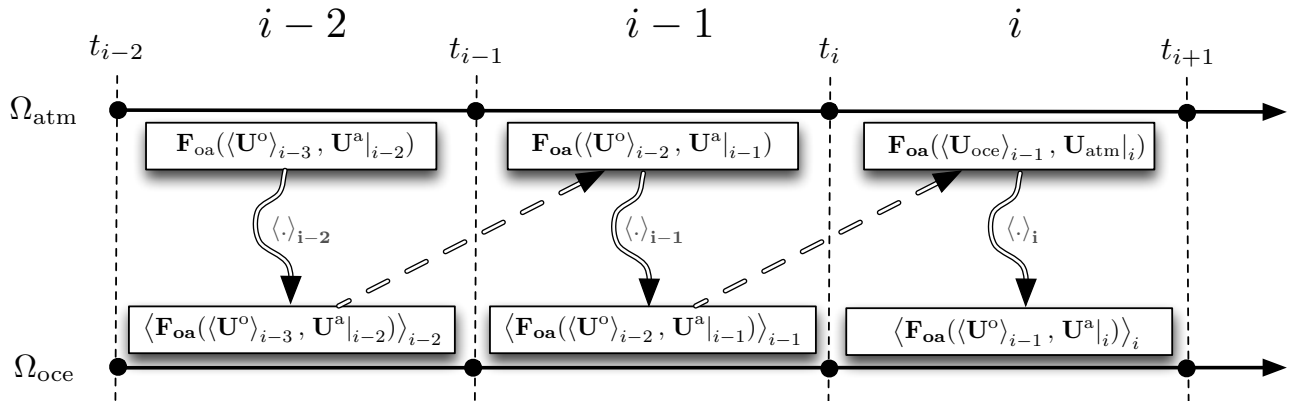


Fig. A2. Schematic view of the coupling by time windows. Three time windows, numbered from $i-2$ to i , are considered here. The arrows correspond to an exchange of information between the two models. The operator $\langle \cdot \rangle_i$ denotes a temporal average over the time window i .

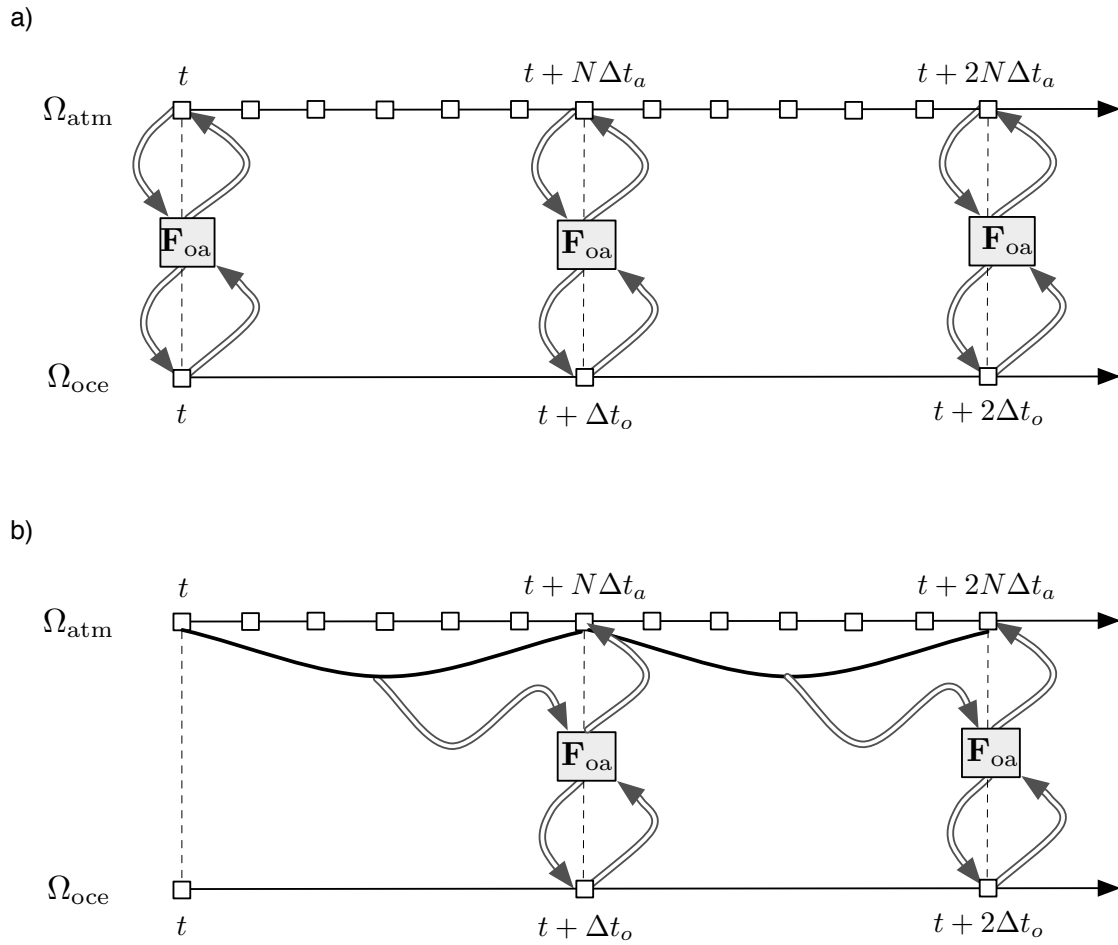


Fig. A3. Example of two coupling strategies at the time step level. Δt_o and Δt_a denote the (baroclinic) time steps respectively of the oceanic and the atmospheric models, with $\Delta t_o = N\Delta t_a$ ($N = 6$ here). The arrows represent an exchange of information with the surface layer parameterization function \mathbf{F}_{oa} . For the atmospheric component this exchange is based on instantaneous values for algorithm a) and on time integrated values for algorithm b).

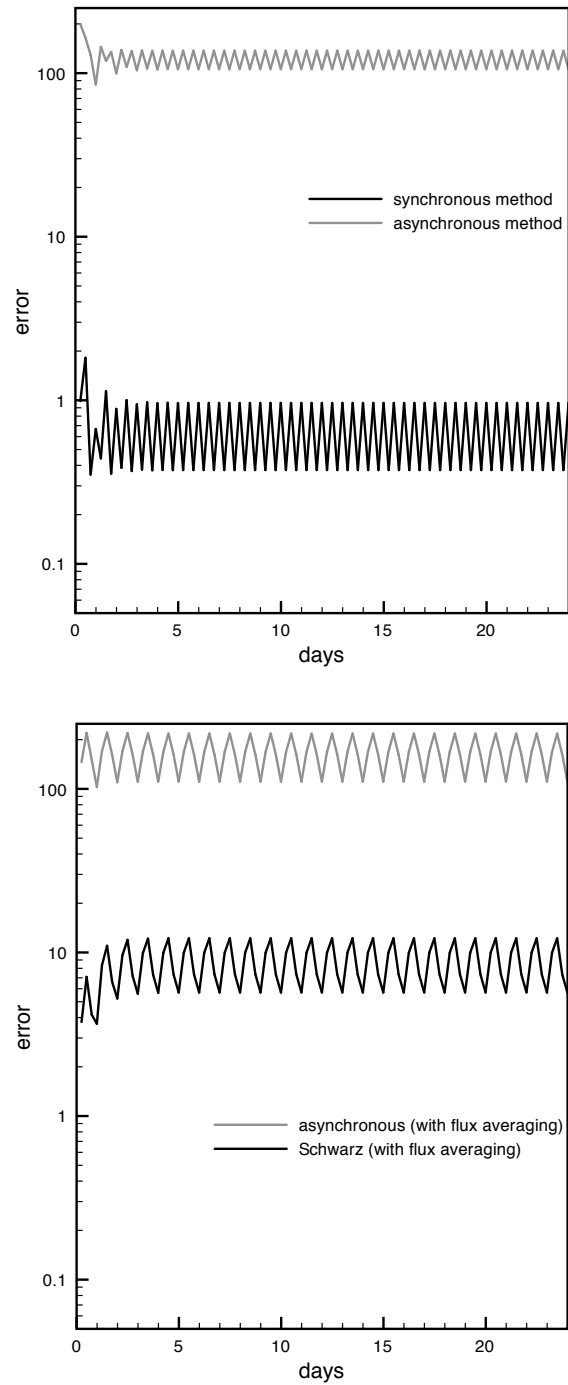


Fig. A4. Time history of the error ℓ_2 -norm for different coupling methods : synchronous and asynchronous methods (left), asynchronous and global-in-time Schwarz methods with flux averaging (right). Note that, whatever the method used, the error ℓ_2 -norm is initially zero because the initial condition satisfies the original equation.

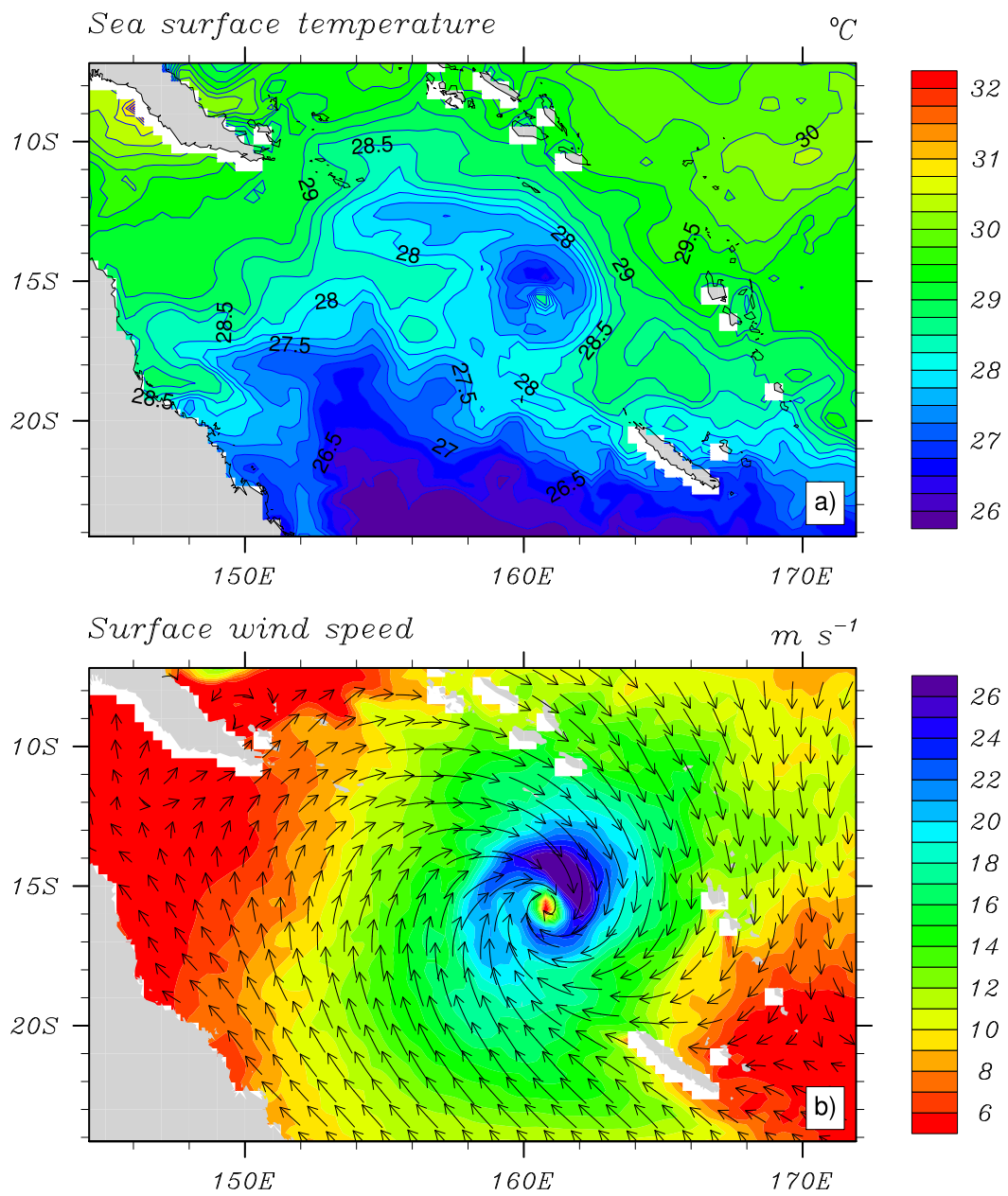


Fig. A5. Snapshots (March 12, 2003 at 8 p.m. GMT) of (a) ROMS sea surface temperature (b) WRF 10 meter winds during a coupled simulation.

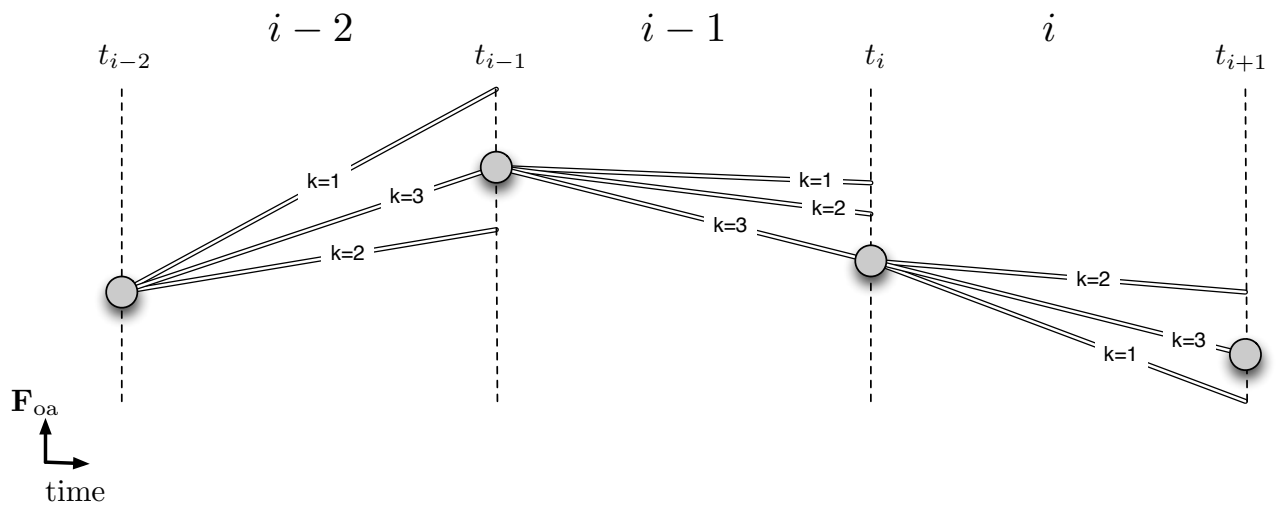


Fig. A6. Piecewise linear reconstruction of the air-sea fluxes for the oceanic model in the case of $N = 3$ iterations. The initial value (grey circles) and the average on a given time-window are sufficient to reconstruct the linear function.

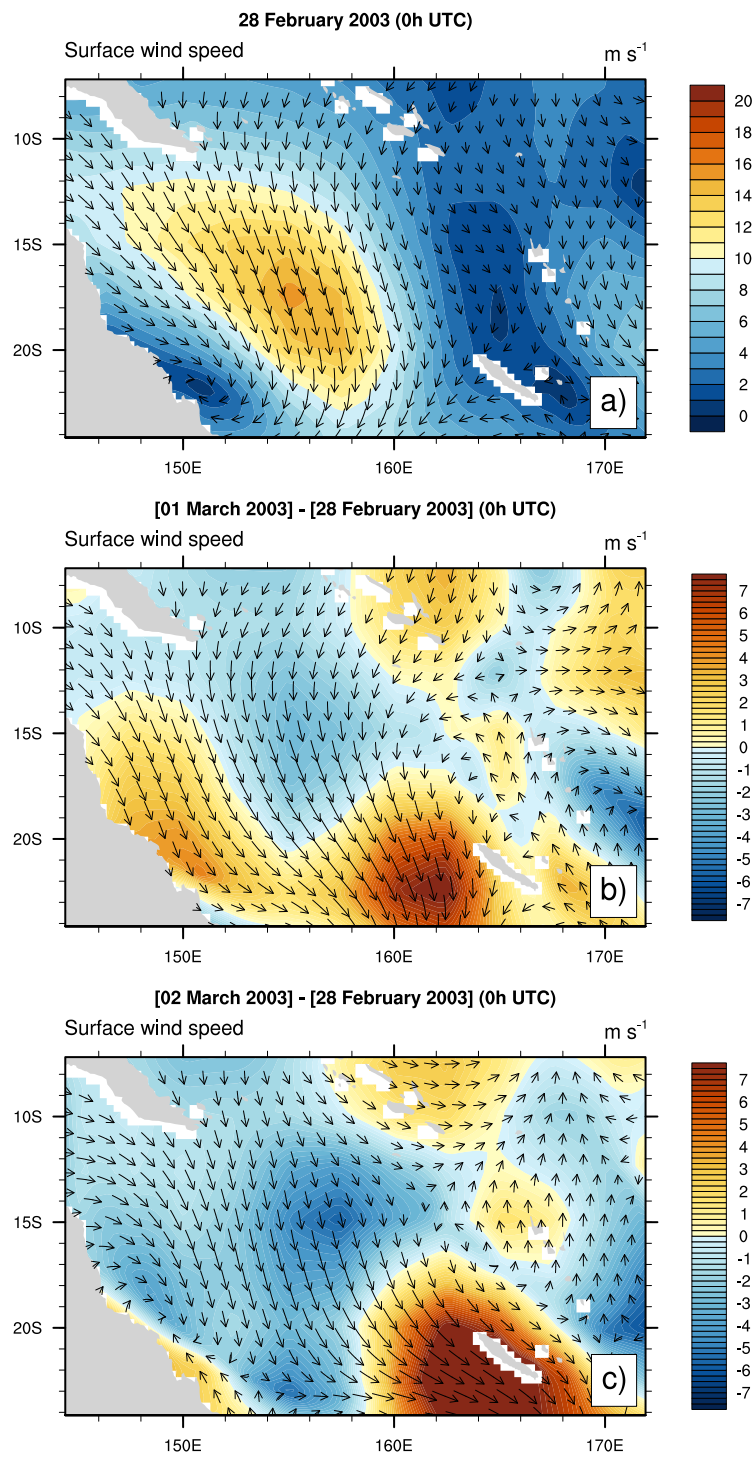


Fig. A7. Initial conditions for the surface winds on 28 Feb. 2003 (a), 01 Mar. 2003 (vectors, b), and 02 Mar. 2003 (vectors, c). Difference in wind speed between Mar. 01 and Feb. 28 (shaded, b), and between Mar. 02 and Feb. 28 (shaded, c)

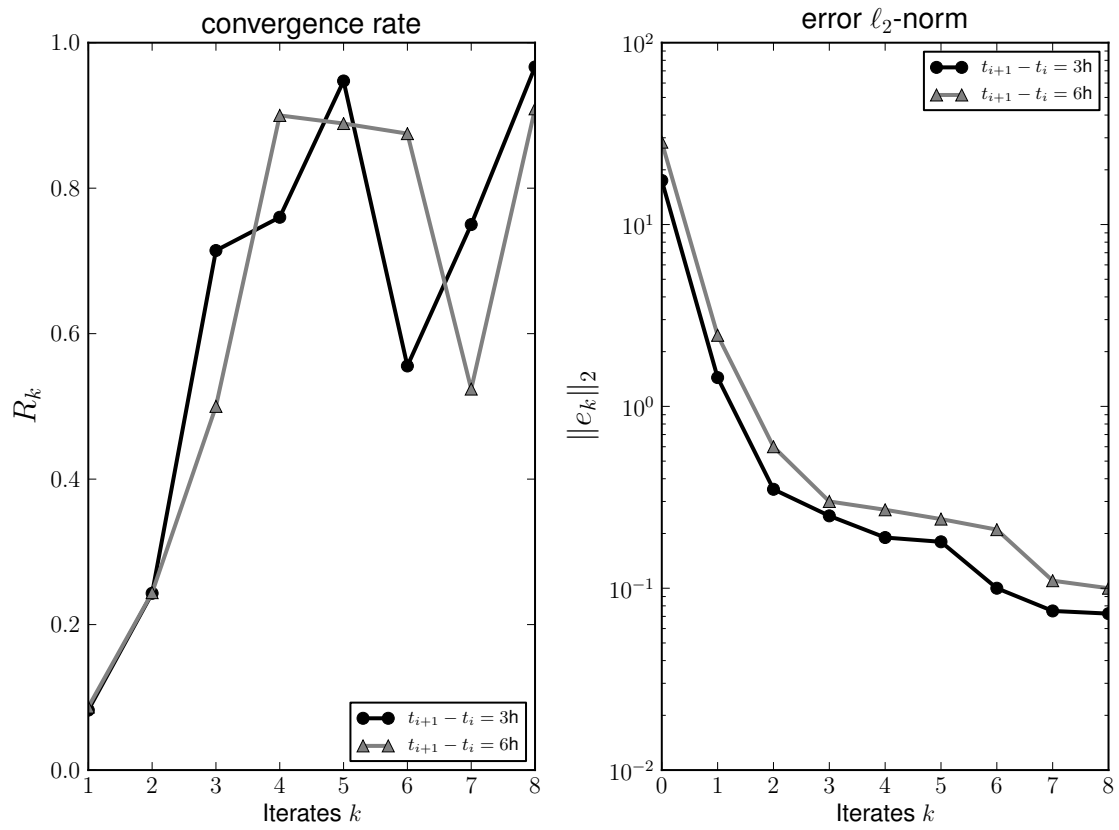


Fig. A8. Ensemble mean of the evolution of the error ℓ_2 -norm (left) and of the convergence rate R_k with respect to the iterates k in the case of time windows of 3 hours and 6 hours. The computation of R_k and $\|e_k\|_2$ is done using sea surface temperature.

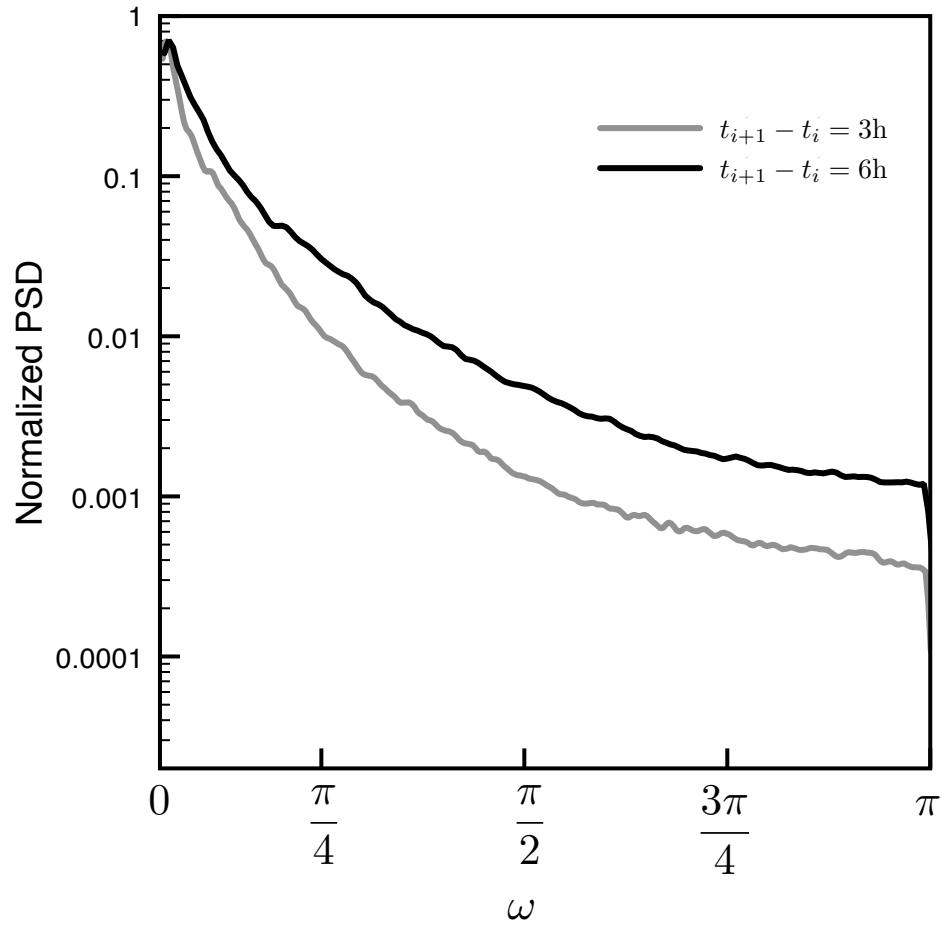


Fig. A9. Ensemble and spatial mean of the normalized power spectral density with respect to ω [h^{-1}] for difference in surface winds between the Schwarz and the asynchronous methods. The computation of Sp_ω is done using low level atmospheric winds.

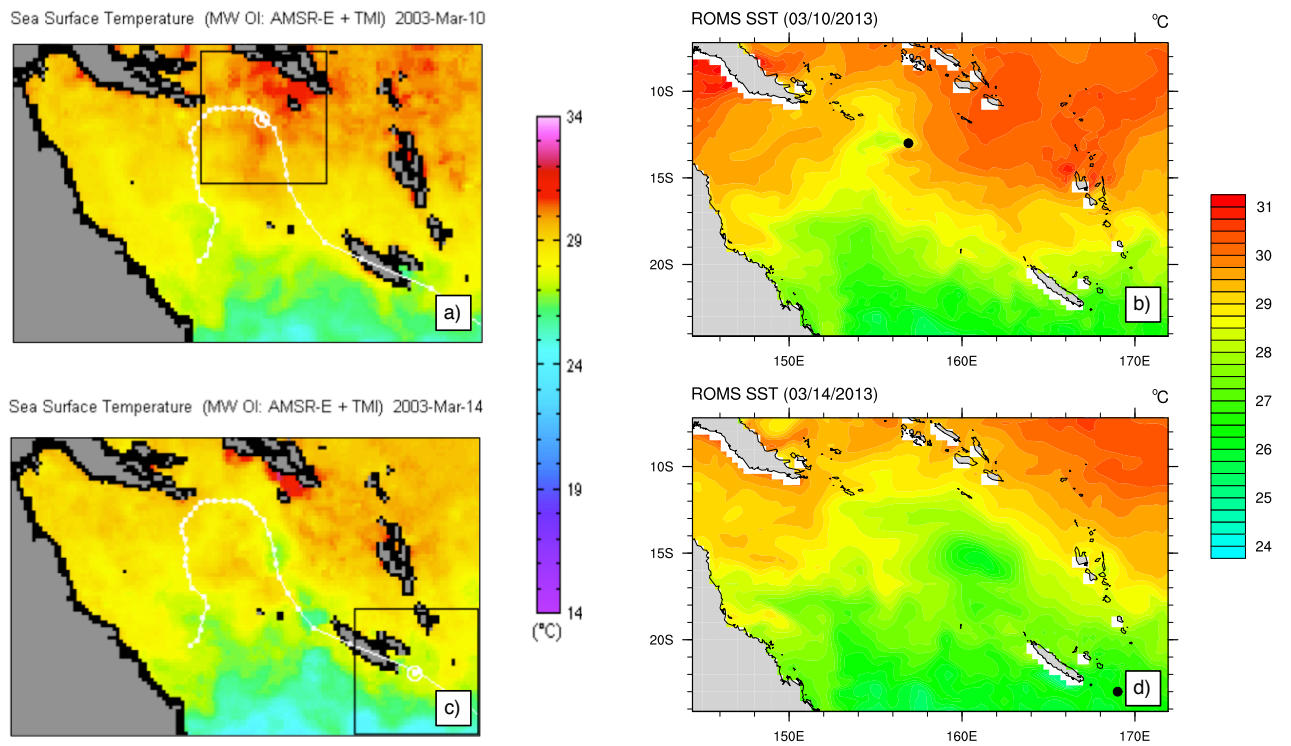


Fig. A10. Observed sea surface temperature [$^{\circ}\text{C}$] (source : <http://www.ssmi.com/>) and cyclone track (white line) for March 10 (a) and March 14 (c). Same for a coupled solution (using the Schwarz method) (b and d). The black dots on b) and d) represent the cyclone eye position.

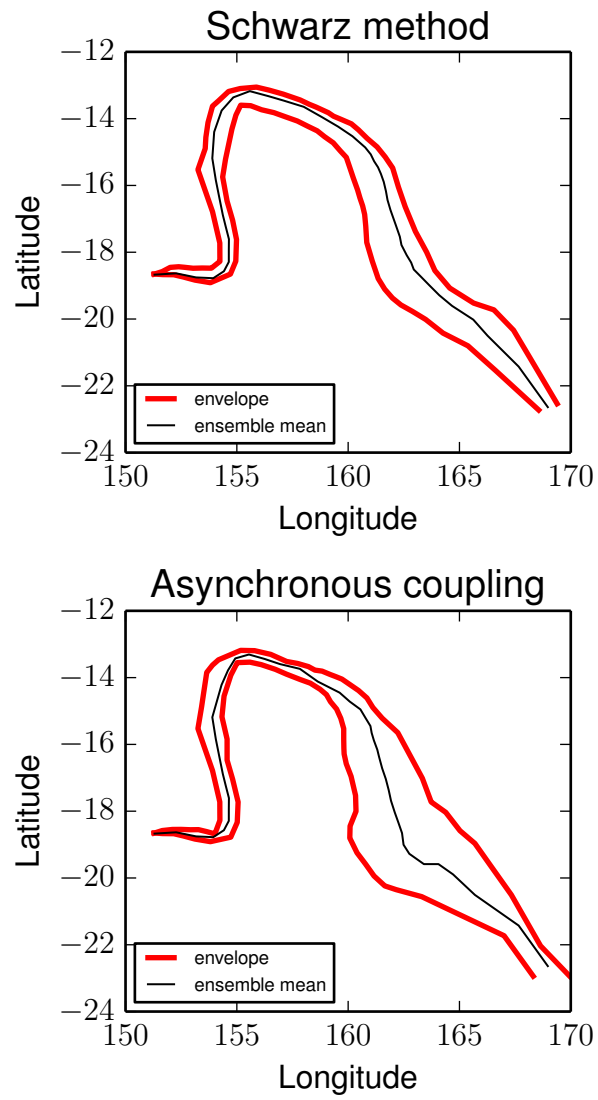


Fig. A11. Ensemble envelopes (thick gray lines) and means (thin black lines) for the cyclone track obtained with the asynchronous method (top) and Schwarz method (bottom) using minimum pressure for the tracking.